# Novel Inorganic (Carbon-Free) Chelate Rings: Tris(chelate) Compounds of [*N*-(Diphenylphosphinoselenoyl)-*P,P*-diphenylphosphinoselenoic amidato-*Se,Se'*] with $M^{III}$ (M = Sb, Bi, In)

**Raymundo Cea-Olivares[a], Verónica García-Montalvo*[a], Josef Novosad[b], J. Derek Woollins[c], Rubén A. Toscano[a], and Georgina Espinosa-Pérez[a]**

Instituto de Química, Universidad Nacional Autónoma de México[a],
Circuito Exterior, Ciudad Universitaria, México 04510, D.F., México
Telefax: (internat.) +52-5-616-2217 or -2203
E-mail: cca@servidor.unam.mx

Department of Inorganic Chemistry, Faculty of Science, Masaryk University[b],
Katlarskas, 61137 Brno, Czech Republic

Department of Chemistry, Loughborough University[c],
Loughborough LE11 3TU, UK

Received December 14, 1995

**Key Words:** Phosphazene metallacycles / [*N*-(Diphenylphosphinoselenoyl)-*P,P*-diphenylphosphinoselenoic amidato-*Se,Se'*] chelates / Inorganic carbon-free chelate rings / Octahedral $MSe_6$ core (M = Sb, Bi, and In)

The $[(SePPh_2)_2N]^-$ ligand **1c** forms stable tris(chelates) with the $Sb^{III}$, $Bi^{III}$, and $In^{III}$ ions. The crystal and molecular structures of the resulting compounds **3**, **4**, and **5** were determined by X-ray diffractometry. The coordination geometry around the metal centers can be described as a distorted octahedron. This feature and the results obtained by comparing the structures with their sulfur and oxygen analogs lead us to conclude that in both $Sb^{III}$ and $Bi^{III}$ compounds the arrangement around the metals suggests a stereochemically nonactive electron lone pair.

Inorganic (carbon-free) chelate rings have enjoyed increasing interest in recent years, since they constitute a bridge between traditional inorganic heterocycles (which contain mainly non-metallic elements) and classical coordination compounds[1]. The anions of the $(PPh_2X)_2NH$ ligands **1** form metal complexes with chelate structures and thus belong to the large family of phosphazene metallacycles. Furthermore, systematic studies of the behavior of this type of ligands suggest that they possess a high degree of ring flexibility and ring bite, as evidenced by the large number of known compounds containing the oxygen (**1a**[2]) and sulfur (**1b**[3]) ligands. In contrast, the selenium-based derivatives **2c** are poorly represented, with only five examples known to date, i.e. those with M = $Re^{V}$[4], $Pd^{II}$, and $Pt^{II}$[5]. Unusual geometries which have already been described include the carbon-free chelate $[Mn\{(SPPh_2)_2N\}_2]$[6], the true square-planar $Te^{II}$ complex with the sulfide ligand **1b**[7], the hexacoordinated lanthanide complexes[8], and more recently the true square-planar $Sn^{II}$ compound with the selenide ligand **1c**, in which the tin lone pair seems to be stereochemically inactive[9].

A recent theoretical study of the stereochemical influence of the lone pair in some hexacoordinated group-15 halides shows that large and electropositive ligands favor the inert pair effect[10]. Given that $(PPh_2X)_2N^-$ ligands offer the opportunity to vary the donor atoms, they provide a unique set of ligands to test the stereochemical influence of the lone pair in main group complexes. Alongside the interest

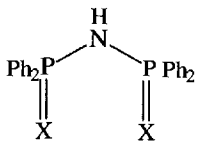

**1**

| | X |
|---|---|
| **a** | O |
| **b** | S |
| **c** | Se |

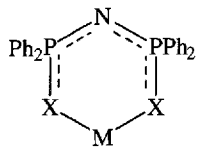

**2**

in preparing new phosphazene heterocycles (**2c**), the structural analyses of the selenium-based compounds of trivalent antimony, bismuth, and indium were undertaken in order to study the effect of variation of the donor group X on the coordination properties by comparing these with their sulfide and oxide analogs[11–13]. We are especially interested in the group-15 derivatives, which may possess a stereoactive electron lone pair and compare to the $In^{III}$ analogs.

## Results and Discussion

The crystalline metal compounds **3**, **4**, and **5** are easily obtained from the corresponding $M^{III}$ chlorides and the potassium salt of **1c**. All of them appear to be air-stable. They are readily soluble in polar organic solvents such as $CHCl_3$ or even in benzene, but insoluble in ethanol and hexane. Their $^{31}P$-NMR spectra at room temperature show that all six phosphorus atoms are equivalent (singlets at $\delta$ =

  0009–2940/96/0808–0919 S 15.00+.25/0 

25.36, 27.25, and 28.51 for **3**, **4**, and **5**, respectively), but no selenium satellites were detectable. In the IR spectra the assignments of the phosphazene bands were relatively easy after identification of the usual phenyl group bands common to the $(PPh_2X)_2N^-$ ligands[2,3]. The individual assignments of the ν(PSe) bands are only partially possible because of overlap with the corresponding γ(PNP) vibrations ($\tilde{\nu}$ = 525–575 $cm^{-1}$). To date, few P–Se vibrations have been clearly assigned[14]. The FAB mass spectra of the compounds exhibit a low-intensity signal for the molecular ion, but rather intense ion fragments resulting from the expected first fragmentations, e.g. $[Se_4(PPh_2)_4N_2Sb^+]$ [*m/z* (%): 1209 (24)], $[Se_4(PPh_2)_4N_2Bi^+]$ [*m/z* (%): 1297 (28)], $[Se_4(PPh_2)_4N_2In^+]$ [*m/z* (%): 1203 (60)]. The base peak in the three spectra is an ion fragment from the ligand, i.e. $[Se(PPh_2)_2N^+]$ (*m/z*: 464), $[Se_2(PPh_2)_2N^+]$ (*m/z*: 544), and $[(PPh_2)_4N^+]$ (*m/z*: 384) for compounds **3**, **4**, and **5** respectively. All of the observed signals exhibit the expected isotopic pattern.

$[Sb\{(SePPh_2)_2N\}_3]$ **3** $[Bi\{(SePPh_2)_2N\}_3]$ **4** $[In\{(SePPh_2)_2N\}_3]$ **5**

### Description of the Structures

Crystallographic data and some solution and refinement parameters are summarized in Table 2[15]. Figure 1 shows the molecular structure and atomic labeling scheme for compound **3**. The molecules **3** and **4** are isostructural. The structure of the indium tris(chelate) **5** is illustrated in the ORTEP plot of Figure 2.

The structures are built up of discrete $[M\{(SePPh_2)_2N\}_3]$ molecules (M = Sb, Bi, and In) in which the coordination geometry around the metal centers can be described as a distorted octahedron[16]. Every metal is coordinated to the selenium atoms of the three bidentate ligands forming six-membered chelate rings. In complexes **3** and **4** the ligands display an asymmetrical chelating coordination mode on interaction with the metal center, resulting in two distinct sets of M–Se bond lengths. The shorter bond lengths correspond to those oriented in the direction of the trigonal face Se(1)–Se(3)–Se(5) [av. M–Se 281(5) and 288(4) pm for **3** and **4**, respectively], and the longer interatomic distances are located towards the opposite face Se(2)–Se(4)–Se(6) [av. M–Se 294(6) and 298(4) pm]. The other bond lengths are consistent with some localization of the bonding, i.e. the bond lengths alternate through the six-membered rings. At the ring side containing the large M–Se bonds [M–Se(2/4/6)] the P–Se bonds are always somewhat shorter relative to the P–Se bonds of the side containing the shorter M–Se bonds [M–Se(1/3/5)]. The two remaining P–N bonds also follow this alternation pattern.

By contrast, the ligands in **5** are coordinated to the indium atom in a symmetrical mode. The average In–Se bond length is 275(5) pm, the difference between the shortest [270.8(3) pm] and the longest [280.7(3) pm] In–Se bond length is only 9.9 pm. The P–N [av. 158.6(9) pm] and P–Se [av. 217.8(7) pm] bond lengths agree well with a π-delocalized structure involving the five ligand atoms in the chelate ring, as has been noted for cyclic phosphazene[17].

Figure 1. ORTEP plot of $[Sb\{(SePPh_2)_2N\}_3]$ (**3**) with thermal ellipsoids at the 50% probability level; hydrogen atoms are omitted for clarity; the bismuth analogue **4** is isostructural. – Selected bond lengths [pm] and angles [°] for **3**/**4**: M–Se(1) 282.4(2)/289.6(3), M–Se(2) 289.0(1)/294.7(2), M–Se(3) 286.3(1)/293.2(2), M–Se(4) 304.2(2)/304.7(3), M–Se(5) 274.2(2)/283.5(3), M–Se(6) 291.5(2)/296.9(3), Se(1)–P(1) 218.7(3)/218.7(5), Se(2)–P(2) 216.6(3)/217.1(6), Se(3)–P(3) 219.4(3)/219.3(5), Se(4)–P(4) 214.4(3)/215.4(5), Se(5)–P(5) 220.2(3)/219.0(6), Se(6)–P(6) 216.8(3)/217.8(5) P(1)–N(1) 158.8(10)/161.0(16), P(2)–N(1) 159.9(12)/157.4(20), P(3)–N(2) 157.0(12)/155.7(18), P(4)–N(2) 160.5(12)/161.3(18), P(5)–N(3) 158.1(12)/158.8(18), P(6)–N(3) 161.1(12)/159.7(17); Se(1)–M–Se(2) 93.8(1)/93.1(1), Se(1)–M–Se(3) 87.2(1)/87.9(1), Se(2)–M–Se(3) 178.9(1)/178.8(1), Se(1)–M–Se(4) 109.4(1)/109.2(1), Se(2)–M–Se(4) 86.9(1)/86.5(1), Se(3)–M–Se(4) 92.5(1)/92.5(1), Se(1)–M–Se(5) 79.9(1)/80.2(1), Se(2)–M–Se(5) 92.5(1)/92.9(1), Se(3)–M–Se(5) 88.0(1)/88.0(1), Se(4)–M–Se(5) 170.7(1)/170.6(1), Se(1)–M–Se(6) 174.7(1)/174.4(1), Se(2)–M–Se(6) 90.2(1)/90.8(1), Se(3)–M–Se(6) 88.8(1)/88.2(1), Se(4)–M–Se(6) 74.2(1)/75.0(1), Se(5)–M–Se(6) 96.5(1)/95.6(1), M–Se(1)–P(1) 108.0(1)/107.7(2), M–Se(2)–P(2), 111.1(1)/110.1(2), M–Se(3)–P(3) 106.2(1)/105.0(2), M–Se(4)–P(4) 106.9(1)/106.5(2), M–Se(5)–P(5) 107.0(1)/106.5(2), M–Se(6)–P(6) 106.4(1)/105.8(2), P(1)–N(1)–P(2) 131.7(7)/132.6(10), P(3)–N(2)–P(4) 133.6(7)/134.0(10), P(5)–N(3)–P(6) 133.3(6)/134.8(9)

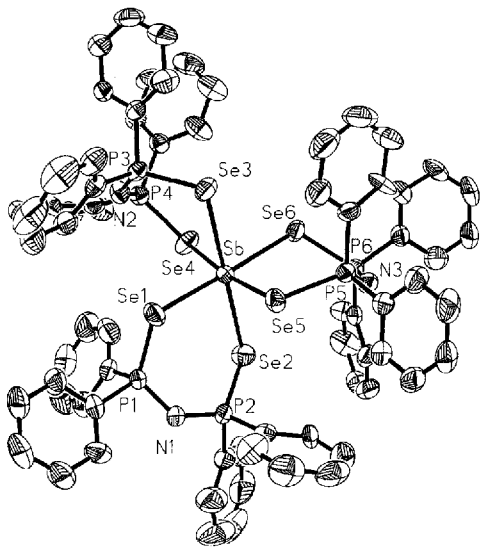


In comparison with the structure of the free ligand **1c**[5], the P–Se bond lengths in these tris(chelates) are considerably increased [**1c**, av. P–Se 209.3(8) pm], whilst the P–N bond lengths are shortened [**1c**, av. P–N 168.2(4) pm] as a consequence of deprotonation and coordination. The Se–P–N angles are also enhanced [**1c**, av. Se–P–N 115.4(9)°], but the P–N–P angles are approximately around the same value [**1c**, av. P–N–P 132.3(2)°].

In each compound, two of the $MSe_2P_2N$ chelate rings are arranged in a distorted boat conformation with selenium and phosphorus atoms at the apices, while the conformation of the other one [that which contains N(2)] can be described as a twisted boat, also with selenium and phosphorus at the apices. Distorted boat conformations were previously observed in the $MSe_2P_2N$ chelate rings from the platinum(II) and palladium(II) derivatives[5]. The twisted boat conformations are also adopted by the $MS_2P_2N$ che-

Figure 2. ORTEP plot of $[In\{(SePPh_2)_2N\}_3]$ (**5**) with thermal ellipsoids at the 50% probability level; hydrogen atoms are omitted for clarity. – Selected bond lengths [pm] and angles [°]: In–Se(1) 270.8(3), In–Se(2) 275.8(2), In–Se(3) 278.7(2), In–Se(4) 277.1(3), In–Se(5) 271.2(3), In–Se(6) 280.7(3), Se(1)–P(1) 218.1(6), Se(2)–P(2) 216.2(5), Se(3)–P(3) 218.7(5), Se(4)–P(4) 217.7(4), Se(5)–P(5) 218.1(6), Se(6)–P(6) 218.2(4), P(1)–N(1) 157.8(16), P(2)–N(1) 160.1(19), P(3)–N(2) 158.9(17), P(4)–N(2) 158.1(17), P(5)–N(3) 158.4(19), P(6)–N(3) 159.0(18); Se(1)–In–Se(2) 97.2(1), Se(1)–In–Se(3) 86.2(1), Se(2)–In–Se(3) 176.5(1), Se(1)–In–Se(4) 100.6(1), Se(2)–In–Se(4) 84.5(1), Se(3)–In–Se(4) 95.5(1), Se(1)–In–Se(5) 84.7(1), Se(2)–In–Se(5) 92.8(1), Se(3)–In–Se(5) 86.9(1), Se(4)–In–Se(5) 174.3(1), Se(1)–In–Se(6) 174.7(1), Se(2)–In–Se(6) 87.2(1), Se(3)–In–Se(6) 89.4(1), Se(4)–In–Se(6) 76.9(1), Se(5)–In–Se(6) 98.0(1), In–Se(1)–P(1) 109.5(2), In–Se(2)–P(2) 109.9(2), In–Se(3)-P(3) 106.6(1), In–Se(4)–P(4) 108.5(2), In–Se(5)–P(5) 107.3(2), In–Se(6)–P(6) 107.1(1), P(1)–N(1)–P(2) 134.3(11), P(3)–N(2)–P(4) 130.5(11), P(5)–N(3)–P(6) 134.5(9)

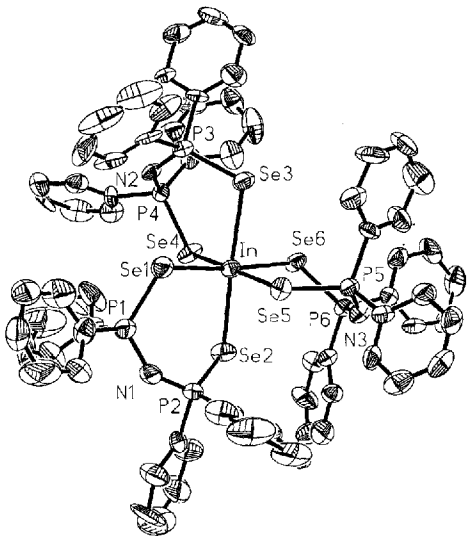


late rings from $Ni^{II}$[5] and $Mn^{II}$[6] complexes. In these conformations the interactions between phenyl groups on different phosphorus atoms but in the same chelate ring are less important than in the chair and boat conformations with the metal and nitrogen atoms at the apices[6]. The average Se···Se bite lengths are 422(4), 428(3), and 413(3) pm for compound **3**, **4**, and **5**, respectively. The other Se···Se nonbonded distances are also longer than the sum of the van der Waals radii[18], and therefore any intramolecular Se···Se contact can be considered.

The packing in the crystal structures is largely determined by van der Waals forces. There are no particularly short intermolecular contacts, the closest intramolecular interactions are some phenyl-phenyl contacts.

On the other hand, some notable structural similarities (Table 1) are observed when the structure **5** is compared with its sulfur and oxygen analogs[12,13], $[In\{(SPPh_2)_2N\}_3]$ and $[In\{(OPPh_2)_2N\}_3]$. The geometry around the indium atom in each derivative exhibits approximately the same octahedral arrangement[19]. The observed deviations might be accounted for by the greater steric crowding in the $InO_6$ core in comparison with that in $InS_6$ and $InSe_6$ coordination spheres, due to shorter In–O bond lengths versus longer In–S bonds, and even longer In–Se bonds, together with the variation of the ring size. The three different ligands are coordinated to the indium atom in a quite symmetrical mode. Only the conformation of the $InX_2P_2N$ chelate rings reveals appreciable differences, as an obvious consequence of the variation of the donor atom X (X = O, S, and Se). The $InO_2P_2N$ and $InS_2P_2N$ chelate rings exhibit a boat and a twisted boat arrangement with the indium and nitrogen atoms at the apices, respectively. This contrasts with the $InSe_2P_2N$ chelate rings, which are arranged in both conformations (boat and twisted boat), but the selenium and the phosphorus atoms are at the apices.

In marked contrast to the observed similiarity between indium compounds, a comparison of the structure of **4** and its sulfur- and oxygen-based analogs[11,13], $[Bi\{(OPPh_2)_2N\}_3]$ and $[Bi\{(SPPh_2)_2N\}_3]$, reveals significant differences (Figure 3). Although each distinct ligand displays a highly asymmetrical chelating coordination mode on interaction with the bismuth atom, the adopted $BiX_6$ coordination geometry is quite different in each case. In $[Bi\{(OPPh_2)_2N\}_3]$, the bismuth assumes a pseudo-trigonally distorted octahedral arrangement exhibiting strong structural evidences for a stereochemically active electron lone pair, while an enigmatic distortion pattern around the central atom was noted in $[Bi\{(SPPh_2)_2N\}_3]$. The $BiSe_6$ coordination geometry in **4** is closer to a $D_{3d}$ symmetry and suggests that the bismuth lone pair is not stereoactive. The resulting arrangement of the $SbSe_6$ core supports the same conclusion: the antimony lone pair appears to be stereochemically inactive. This may be explained by the presence of larger and more electropositive donor atoms, as has been pointed out by the frontier orbital arguments for the hexacoordinated group-15 halides[10]. For electropositive central atoms and sufficiently electropositive ligands, the small HOMO-$1a_1$ energy gap controls the distortion and favors the "inert pair effect". In agreement with this fact, most of the tin(II) compounds are also known to possess distorted geometries with a stereoactive lone pair, unless the tin atom is surrounded by easily polarizable anions, e.g. SnSe and SnTe. In this last case a regular geometry around the tin atom is observed[20]. This led us to conlude that the observed distortion pattern of the $BiS_6$ core noted in $[Bi\{(SPPh_2)_2N\}_3]$ might be an intermediate case. Additionally, the results obtained by comparing the structures of indium compounds can be used to assess the degree of the steric influence of the ligands on the coordination sphere in the absence of the electron lone pair. In spite of the great size differences between the donor atoms (X = O, S, and Se) and consequently between the chelate rings, the resulting similar $InX_6$ coordination geometries are remarkable. This contrasts with the observed differences in the corresponding $BiX_6$ arrangement. Furthermore, the variation observed in the average P–N–P, M–X–P, X–P–N angles and in the ring bite (X···X) for the compounds described in this paper and for their sulfur and oxygen analogs (Table 1) demonstrates the high flexibility of this type of phosphazenoid ligands as well as their ability to fulfill the requirements imposed by the central atom and their notable chelating capacity.

Table 1. Average interatomic distances [Å] and angles [°] in some chelate rings containing $\{(XPPh_2)_2N\}$ ligands **1** (X = O, S, and Se)[a]

| Compound | M-X | P-X | P-N | X···X bite | X-M-X bite | M-X-P | X-P-N | P-N-P |
|---|---|---|---|---|---|---|---|---|
| $[Sb\{(SePPh_2)_2N\}_3]$, **(3)**[b] | 288(9) | 217(2) | 159(1) | 422(4) | 94.2(1.6) | 107.6(1.6) | 118.8(1.2) | 132.8(8) |
| $[Bi\{(SePPh_2)_2N\}_3]$, **(4)**[b] | 293(6) | 218(1) | 158(2) | 428(3) | 93.73(1.3) | 106.9(1.6) | 119.0(1.6) | 133.8(9) |
| $[Bi\{(SPPh_2)_2N\}_3]$ [c] | 282(8) | 201(1) | 159.3(4) | 397(8) | 89.5(4.0) | 103.0(2.7) | 118.5(1.0) | 134.1(1.6) |
| $[Bi\{(OPPh_2)_2N\}_3]$ [d] | 233(5) | 152.0(6) | 157.8(4) | 310(6) | 83.4(1.0) | 129.5(2.5) | 117.4(9) | 130.4(1.8) |
| $[In\{(SePPh_2)_2N\}_3]$, **(5)**[b] | 275(3) | 217.8(7) | 158.6(9) | 413(3) | 96.8(9) | 108.1(1.2) | 118.7(9) | 133.1(1.7) |
| $[In\{(SPPh_2)_2N\}_3]$ [e] | 263(3) | 202(3) | 156(6) | 378(6) | 91.9(1.6) | 106.8(1.8) | 118.3(1.7) | 139.8(4.1) |
| $[In\{(OPPh_2)_2N\}_3]\ C_6H_6$ [d] | 212.7(9) | 151.5(4) | 158.4(7) | 299(2) | 89.6(7) | 126.7(1.0) | 117.3(4) | 127.0(4) |

[a] All datas are weighted averages. – [b] This study. – [c] See ref.[11]. – [d] See ref.[13]. – [e] See ref.[12].

Figure 3. Model fitting view of the $BiX_6$ core with X = O, S, and Se

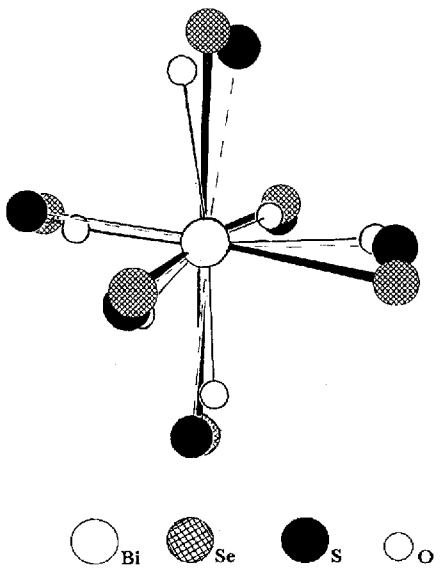


We are grateful to *DGAPA-UNAM* (Grant IN100395) for financial support. V. G. M. and J. N. acknowledge *Mexican National Council of Science and Technology* (CONACYT) for generous support and thank *L. Velasco-Ibarra* and *F. J. Pérez-Flores* for their work in recording FAB MS.

## Experimental

$^{31}P$ NMR: Varian VXR 300s spectrometer, 121 MHz (with $H_3PO_4$, 85%, as reference). – FAB MS (3-nitrobenzyl alcohol support): Jeol JMS-SX102A, positive-ion mode. – IR (KBr): Perkin-Elmer 283B. – Microanalyses: Galbraith Laboratories. – Bis(diphenylphosphinoselenoyl)amide (**1c**), prepared by the method of Woollins et al.[5], was converted to its potassium salt by the reaction with KO*t*Bu according to a previously described procedure[21].

*Tris[N-(diphenylphosphinoselenoyl)-P,P-diphenylphosphinoselenoic amidato-Se,Se']antimony(III)* $[Sb\{(SePPh_2)_2N\}_3$, **3**]: A solution of $SbCl_3$ (0.045 g, 0.2 mmol) in 5 ml of THF was added to a solution of $[K(SePPh_2)_2N]$ (0.348 g, 0.6 mmol) in 5 ml of methanol. The precipitated orange solid was filtered, washed with methanol and dried in vacuo. Yield 0.230 g (66%). Suitable crystals for X-ray diffraction were grown by allowing a layer of *n*-hexane to diffuse slowly into a solution of **3** in dichloromethane at room temp. – $^{31}P$ NMR ($CDCl_3$): δ = 29.4 (s). – IR (KBr): $\tilde{\nu}$ = 3052 $cm^{-1}$ m [ν(CH)]; 1203 s, br [ν(P–N)] + 1177 s [ν(P–N)/δ(CH)]; 743 m [ν(P–N)]; 689 vs [Φ(CC), Ph]; 527 vs [γ(PNP)/ν(P–Se)]; 437 w-m [ν(P–Se)]. – MS ($FAB^+$, $CH_3Cl$, for $^{80}Se$ and $^{121}Sb$), *m/z*: 1209 $[Se_4(PPh_2)_4N_2Sb^+]$, 1129 $[Se_3(PPh_2)_4N_2Sb^+]$, 665 $[Se_2(PPh_2)_2NSb^+]$, 544 $[Se_2(PPh_2)_2N^+]$, 464 $[Se(PPh_2)_2N^+]$, 384 $[(PPh_2)_4N^+]$. – $C_{72}H_{60}N_3P_6SbSe_6$ (1748.7): calcd. C 49.46, H 3.46; found C 48.93, H 3.50.

*Tris[N-(diphenylphosphinoselenoyl)-P,P-diphenylphosphinoselenoic amidato-Se,Se']bismuth(III)* $[Bi\{(SePPh_2)_2N\}_3$, **4**] was prepared by adding a solution of 0.348 g (0.6 mmol) of $[K(SePPh_2)_2N]$ in 10 ml of methanol with stirring to a solution of 0.063 g (0.2 mmol) of $BiCl_3$ in THF. The resulting red-orange precipitate was filtered, washed with ethanol and dried in vacuo. Yield 0.268 g, (73%). Crystals suitable for X-ray crystallography were obtained by solvent diffusion in a dichlorometane/*n*-hexane mixture at room temp. – $^{31}P$ NMR ($CDCl_3$): δ = 27.25 (s). – IR (KBr): $\tilde{\nu}$ = 3051 $cm^{-1}$ m [ν(CH)]; 1203 s, br [ν(P–N)] and 1177 s [ν(P–N)/δ(CH)]; 742 m [ν(P–N)]; 691 vs [Φ(CC), Ph]; 531 vs [γ(PNP)/ν(P–Se)]; 441 w-m [ν(P–Se)], 382 w [ν(Se–P–N)]. – MS ($FAB^+$, $CH_3Cl$, for $^{80}Se$), *m/z*: 1841 $[M^+]$, 1297 $[Se_4(PPh_2)_4N_2Bi^+]$, 1217 $[Se_3(PPh_2)_4N_2Bi^+]$, 753 $[Se_2(PPh_2)_2NBi^+]$, 544 $[Se_2(PPh_2)_2N^+]$, 464 $[Se(PPh_2)_2N^+]$, 384 $[(PPh_2)_4N^+]$. – $C_{72}H_{60}BiN_3P_6Se_6$ (1835.9): calcd. C 47.11, H 3.29; found C 46.62, H 3.17. – Mol. mass 1841 (FAB MS; $CH_3Cl$, for $^{80}Se$).

*Tris[N-(diphenylphosphinoselenoyl)-P,P-diphenylphosphinoselenoic amidato-Se,Se']indium(III)* $[In\{(SePPh_2)_2N\}_3$, **5**]: To a solution of 0.348 g (0.6 mmol) of $[K(SePPh_2)_2N]$ in 5 ml of meth-

Table 2. Crystallographic data of the complexes **3**, **4**, and **5**

| | **3** | **4** | **5** |
|---|---|---|---|
| Formula | $C_{72}H_{60}N_3P_6Se_6Sb$ | $C_{72}H_{60}N_3P_6Se_6Bi$ | $C_{72}H_{60}N_3P_6Se_6In$ |
| Formula mass | 1748.6 | 1835.8 | 1741.6 |
| Color, habit | orange, prism | red, prism | light-yellow, plates |
| Cryst. size, [mm] | 0.44x 0.28x 0.20 | 0.28x 0.20x 0.18 | 0.32x 0.24x 0.06 |
| *F*(000) | 1716 | 1780 | 1712 |
| Space group | *P*-1 | *P*-1 | *P*-1 |
| Crystal system | triclinic | triclinic | triclinic |
| *a* [pm] | 1154.8 (1) | 1154.2 (2) | 1159.1 (1) |
| *b* [pm] | 1324.4 (1) | 1322.6 (2) | 1319.1 (1) |
| *c* [pm] | 2473.3 (2) | 2489.6 (2) | 2486.3 (2) |
| α [°] | 97.695 (5) | 97.67 (2) | 98.986 (6) |
| β [°] | 96.705 (6) | 97.01 (2) | 96.360 (9) |
| γ [°] | 109.649 (5) | 109.28 (2) | 110.284 (6) |
| *V* [$nm^3$] | 3.4771 (6) | 3.4988 (9) | 3.4655 (8) |
| *Z* | 2 | 2 | 2 |
| $\rho_{calcd}$ [$mg/cm^3$] | 1.670 | 1.743 | 1.669 |
| Scan type | ω | ω | ω |
| 2θ range [°] | 3.0 - 50.0 | 3.0 - 50.0 | 3.0 - 50.0 |
| Scan speed [°/min] | 3.00 - 60.00 | 4.00 - 100.00 | 3.00 - 100.00 |
| Reflections collected | 12733 | 13079 | 12737 |
| Independent | 12082 | 12172 | 12078 |
| Observed reflections | 6743 [$F>4.0\sigma(F)$] | 5559 [$F>4.0\sigma(F)$] | 5181 [$F>4.0\sigma(F)$] |
| μ [$mm^{-1}$] | 3.719 | 5.822 | 3.675 |
| Absortion correction | Face-indexed | ψ scan | Face-indexed |
| Min./max. | 0.3487/0.5241 | 0.2601/0.3783 | 0.4223/0.8058 |
| Parameters refined | 794 | 794 | 794 |
| $R(F_o)$ % | 5.74 | 6.13 | 6.61 |
| $Rw(F_o)$ % | 6.02 | 6.12 | 6.85 |
| Goodnes-of-fit | 1.12 | 1.06 | 1.06 |

anol an aqueous solution of 0.044 g (0.2 mmol) of $InCl_3$ in 5 ml of water was added. A light yellow product precipitated immediately and was filtered by suction and washed with water and methanol. Yield 0.264 g (76%). Suitable crystals for X-ray diffraction were grown by allowing a layer of *n*-hexane to diffuse slowly into a solution of **5** in dichloromethane at room temp. – $^{31}P$ NMR ($CDCl_3$): $\delta$ = 28.5 (s). – IR (KBr): $\tilde{\nu}$ = 3052 $cm^{-1}$ m [$\nu$(CH)]; 1209 s, br [$\nu$(P–N)] and 1177 s [$\nu$(P–N)/$\delta$(CH)]; 743 m [$\nu$(P–N)]; 689 vs [$\Phi$(CC), Ph]; 531 vs [$\gamma$(PNP)/$\nu$(P–Se)]. – MS (FAB$^+$, $CH_3Cl$, for $^{80}Se$ and $^{115}In$), *m/z*: 1747 [$M^+$], 1203 [$Se_4(PPh_2)_4N_2In^+$], 1123 [$Se_3(PPh_2)_4N_2In^+$], 659 [$Se_2(PPh_2)_2NIn^+$], 544 [$Se_2(PPh_2)_2N^+$], 464 [$Se(PPh_2)_2N^+$], 384 [$(PPh_2)_4N^+$]. – $C_{72}H_{60}InN_3P_6Se_6$ (1741.7): calcd. C 49.65, H 3.47; found C 48.90, H 3.52. – Mol. mass 1747 (FAB MS; $CH_3Cl$, for $^{80}Se$ and $^{115}In$).

*X-ray Structure Determination:* Data collections were performed at room temp. with a Siemens P4 four-cycle diffractometer by using graphite monochromated Mo-$K_\alpha$ radiation ($\lambda$ = 0.71073 Å). Table 2 compiles the data for the structure determinations. The structures were solved by direct methods using Siemens SHELXTL-PLUS (PC version)[22] and refined by full-matrix least-squares calculation. All non-hydrogen atoms were refined anisotropically. Hydrogen atoms were calculated as a riding model with fixed isotropic $U$ = 0.08.


[1] I. Haiduc, I. Silaghi-Dimitrescu, *Coord. Chem. Rev.* **1986**, *74*, 127–270.

[2] I. Haiduc, C. Silvestru, H. W. Roesky, H.-G. Schmidt, M. Noltemeyer, *Polyhedron* **1993**, *12*, 69–75; J. S. Casas, I. Haiduc, A. Sánchez, J. Sordo, E. M. Vázquez-López, *ibid.* **1994**, *13*, 2873–2879, and references cited therein.

[3] R. O. Day, R. R. Holmes, A. Schmidpeter, K. Stoll, L. Howe, *Chem. Ber.* **1991**, *124*, 443–448; C. Silvestru, R. Cea-Olivares, I. Haiduc, A. Zimbron, *Polyhedron* **1994**, *13*, 159–165, and references cited therein.

[4] R. Rossi, A. Marchi, L. Marvelli, L. Margon, M. Peruzzini, U. Casellato, R. Graziani, *J. Chem. Soc., Dalton Trans.* **1993**, 723–729; R. Rossi, A. Marchi, L. Marvelli, M. Peruzzini, U. Casellato, R. Graziani, *ibid.* **1993**, 723–729.

[5] P. Bhattacharyya, J. Novosad, J. Phillip, A. M. Z. Slawin, D. J. Williams, J. D. Woollins, *J. Chem. Soc., Dalton Trans.* **1995**, 1607–1613.

[6] O. Siiman, H. B. Gray, *Inorg. Chem.* **1974**, *13*, 1185–1191.

[7] S. Bjornevag, S. Husebye, K. Maartmann-Moe, *Acta Chem. Scand., Ser. A*, **1982**, *36*, 195–202.

[8] I. Rodríguez, C. Alvarez, J. Gómez-Lara, R. Cea-Olivares, *Lanthanide Actinide Res.* **1985–6**, *1*, 253.

[9] R. Cea-Olivares, V. García-Montalvo, J. Novosad, J. D. Woollins, G. Espinosa-Pérez, *J. Chem. Soc., Chem. Commun.* **1996**, 519–520.

[10] R. A. Wheeler, P. N. V. P. Kumar, *J. Am. Chem. Soc.* **1992**, *114*, 4776–4784.

[11] D. J. Williams, C. O. Quicksall, K. M. Barkigia, *Inorg. Chem.* **1982**, *21*, 2097–2100.

[12] R. Cea-Olivares, R. A. Toscano, G. Carreón, J. Valdés-Martínez, *Monatsh. Chem.* **1992**, *123*, 391–396.

[13] V. García-Montalvo, R. Cea-Olivares, D. J. Williams, G. Espinosa-Pérez, *Inorg. Chem.*, in press.

[14] V. Krishnan, R. A. Zingaro, *Inorg. Chem.* **1969**, *8*, 2337–2340; J. Ellermann, A. A. M. Demuth, W. Bauer, *Z. Naturforsch., B: Anorg. Chem., Org. Chem.* **1986**, *41*, 863; J. Ellermann, J. Sutler, F. A. Knoch, M. Moll, *Chem. Ber.* **1994**, *127*, 1015–1020.

[15] Further details of the crystal structure investigations are available from the Fachinformationszentrum Karlsruhe, D-76344 Eggenstein-Leopoldshafen (Germany), on quoting the depository numbers CSD-404978 (**3**), -404923 (**4**), and -404977 (**5**), the names of the authors and the journal citation.

[16] According to the dihedral angle ($\delta'$) criterion, our tris(chelates) are close to the $D_{3d}$ limit from the path $O_h(D_{3d}) \leftrightarrow D_{3h}$ [ideal $\delta'$ angles: $O_h(D_{3h})$ 70.5, 70.5, 70.5° at $b_1$ and 70.5, 70.5, 70.5° at $b_2$ $O_h(D_{3h}) \leftrightarrow (D_{3h})$ 0, 0, 0° at $b_1$ and 120, 120, 120° at $b_2$]. The observed $\delta'$ angles are 71.5, 65.6, 106.3° at $b_1$, and 101.5, 68.9, 76.4° at $b_2$ for **3**; 71.1, 65.4, 105.8° at $b_1$, and 102.5, 68.5, 75.8° at $b_2$ for **4**, 65.1, 68.8, 107.0° at $b_1$, and 104.8, 72.8, 75.8° at $b_2$ for **5**. E. L. Muetterties, L. J. Guggenberger, *Inorg. Chem.* **1974**, *96*, 1748–1756.

[17] R. Allcock, *Phosphorus-Nitrogen Compounds*, Academic Press, New York, **1972**, Chapter 3.

[18] A. Bondi, *J. Phys. Chem.* **1964**, *68*, 441–451.

[19] The observed dihedral $\delta'$ angles are 65.1, 68.8, 107.0° at $b_1$, and 104.8, 72.8, 75.8° at $b_2$ for **5**; 71.0, 70.1, 108.4° at $b_1$, and 111.0, 71.5, 72.5° at $b_2$ for [In{$(OPPh_2)_2N$}$_3$]; 72.1, 78.1, 110.0° at $b_1$, and 113.3, 67.7, 67.2° at $b_2$ for [In{$(SPPh_2)_2N$}$_3$]. See ref.[11].

[20] M. Veith, O. Recktenwald, *Top. Curr. Chem.* **1982**, *104*, 1–55.

[21] A. Schmidpeter, H. Groeger, *Z. Anorg. Allg. Chem.* **1966**, *345*, 106.

[22] Siemens SHELXTL PLUS, Release 4.0 for Siemens R3 Crystallographic.


[95206]